PROCEEDINGS OF SCIENCE

Considering the importance of gamma-gamma absorption in gamma-ray binaries

Brian van Soelen[a,*] **and Drikus du Plooy**[a]

[a] *University of the Free State,*
205 Nelson Mandela Drive, Bloemfontein, South Africa

E-mail: vansoelenb@ufs.ac.za

Gamma-ray binaries are a rare subclass of high mass binary systems, where the non-thermal emission peaks in the gamma-ray regime. Two scenarios have been proposed to explain the production of the emission; in the pulsar wind scenario the compact object is proposed to be a rapidly rotating pulsar, and the emission originates from particle acceleration that occurs at the shock that forms between the pulsar and stellar wind; in the microquasar scenario emission originates from a relativistic jet. In the pulsar wind scenario, the particle acceleration is normally assumed to occur at the apex of the shock, but hydrodynamic simulations have shown that a second shock could occur due to Coriolis forces. Since gamma-gamma absorption will strongly attenuate TeV emission originating from the apex of the shock, this may imply that it originates from this second shock region. We have undertaken a full calculation of the gamma-gamma optical depth around the gamma-ray binary LS 5039, to investigate whether gamma-gamma absorption may introduce observable features that could be used to constrain the location of the gamma-ray production.

**** High Energy Astrophysics in Southern Africa (HEASA2021) ****
**** 13 - 17 September, 2021 ****
**** Online ****

[*] Speaker

PoS(HEASA2021)028

1. Introduction

A small number (< 10) of high mass binary systems show persistent non-thermal emission which peaks (in a νF_ν distribution) at gamma-ray energies. Collectively know as gamma-ray binaries, these sources are observed up to TeV energies, and show variable emission on their orbital periods. All sources consist of an O or Oe/Be type star with a compact object in the mass range of a neutron star or black hole [see e.g. 1, 2]. For two sources, PSR B1259-63 and PSR J2032+4127, pulsed radio and/or gamma-ray emission has been detected, indicating the compact object is a pulsar [3, 4]. While a pulsed signal has not been detected from the other sources, they all have smaller binary separations, and the pulsed radio emission would be absorbed in the stellar wind [e.g. 5]. A microquasar and pulsar wind scenario have been proposed to explain the observed emission. In the microquasar scenario, the gamma-ray emission originates from a relativistic jet, while in the pulsar wind scenario the emission arises from the interaction of the shock that forms between the pulsar and stellar wind [see e.g. 1, 2, and references therein]. The similarity between gamma-ray binaries, favours the idea that all systems are powered by a young pulsar, but arguments can still be made for a microquasar scenario [e.g. 6].

In the pulsar wind scenario the majority of the emission is often assumed to originate from the apex of the shock that forms between the pulsar and stellar wind, but hydrodynamic simulations have shown the formation of a secondary shock further out [7, 8] which suggests a second location for the production of very high energy gamma-rays [9]. Since gamma-ray emission is assumed to be produced by inverse Compton scattering of the photons from the companion star, this same photon field will be a target for very high energy gamma-rays which would be attenuated by gamma-gamma absorption [as previously investigated by, e.g. 10, 11]. The magnitude of the gamma-gamma absorption, and the influence it will have on the shape of the high energy and very high energy spectrum, depends on the distance of the gamma-ray emission region from the companion star and we are, therefore, investigating whether this may introduce an observable signature that could be used to constrain the location of the gamma-ray production region. Here we present initial results from this investigation, considering the results for LS 5039.

2. Gamma-gamma absorption

The optical depth of a gamma ray of energy E_γ, due to gamma-gamma absorption is given by [12]

$$\tau_{\gamma\gamma} = \int_0^\infty d\ell \int_0^{4\pi} d\Omega \int_{\frac{2}{E_\gamma(1-\mu)}}^\infty d\epsilon\, n_\epsilon(\epsilon,\Omega)\sigma_{\gamma\gamma}(\epsilon, E_\gamma, \mu)(1-\mu) \tag{1}$$

where ℓ is the distance over which the gamma ray should travel, Ω is the solid angle over the target photon field, ϵ is the energy of the target photons, $\mu = \cos\theta$ where θ is angle between the gamma ray and target photon directions of propagation, $n_\epsilon(\epsilon,\Omega)$ is the number density of the target photons, and the cross-section, $\sigma_{\gamma\gamma}$ is given by

$$\sigma_{\gamma\gamma}(\beta) = \frac{3}{16}\sigma_{\rm T}\left(1-\beta^2\right)\left[(3-\beta^4)\ln\left(\frac{1+\beta}{1-\beta}\right) - 2\beta(2-\beta^2)\right] \tag{2}$$

where

$$\beta = \sqrt{1 - \frac{2}{\epsilon E_\gamma (1-\mu)}}. \tag{3}$$

We assume that the target photons originate from the companion star, and and their spectrum is described by a blackbody distribution. The gamma-gamma absorption is calculated by considering the interactions over all solid angles, assuming the star is a sphere.

3. Inverse Compton Spectrum

The inverse Compton emission was calculated using the approximation given by [13] as implemented in the NAIMA package [14]. A power-law with exponential cut-off electron spectrum was used, which was assumed to remain the same at all phases. As with the gamma-gamma absorption, the photon field is assumed to be the blackbody radiation provided by the companion star. Unlike the gamma-gamma absorption, we assume the star is a point-like source, and the scattering is calculated at only a single angle, at each orbital phase.

4. Results

The gamma-gamma absorption has been calculated for the region around the gamma-ray binary LS 5039, up to 20 times the binary separation. This system consists of a O6.5 V((f)) star and unknown compact object, in a 3.90603 day orbit ($e = 0.24$) [15, 16]. Adopting the solution from [16], the phases of inferior and superior conjunction are $\phi_{\rm inf} = 0.64$ and $\phi_{\rm sup} = 0.06$, respectively. The absorption maps are shown in figure 1 for an inclination angle of $i = 13°$ and $i = 64°$. Since the measured mass-function for the system is $f = 0.0049\,{\rm M}_\odot$ [16], for an assumed mass for the O star of $22.9\,{\rm M}_\odot$ [15], this corresponds to a mass for the compact object of $M_c = 7.3\,{\rm M}_\odot$ and $M_c = 1.6\,{\rm M}_\odot$, respectively. For the smaller inclination angle, the absorption remains similar throughout the orbit, while for the higher inclination angle, the absorption changes from negligible near inferior conjunction to over 90% absorption around superior conjunction.

We modelled the very high energy light curve via inverse Compton scattering assuming an inclination of $i = 64°$ (neutron star compact object), calculating the light curve assuming the emission is produced at the stand-off shock and at a point at 15 times the binary separation. The electron spectrum was normalized such that the shape of the modelled flux, after absorption, matched the observed spectrum around inferior conjunction (figure 2).

The modelled light curve (normalized) is shown in figure 3 (left column), compared to the observed very high energy flux [18]. In the case that the gamma-ray emission region is located at the stand-off shock, the flux peaks around phase ~ 0.79 (inferior conjunction at $\phi_{\rm inf} = 0.77$), similar to the observed light curve. If the emission region is located at 15 times the binary separation, the attenuation due to gamma-gamma absorption is much lower, and the flux peaks at phase ~ 0.96, near periastron, in contradiction to the observations. The effect on the spectrum is shown in the middle column of figure 3, for five representative phases. For the emission produced at the shock-front, the spectrum is highly absorbed around $E_\gamma = 1\,{\rm TeV}$, significantly changing the shape, while the influence is far less noticeable at greater distances. The predicted photon index, found by fitting a power-law to the modelled spectrum between 0.2 and 5 TeV, is shown in the right hand column of

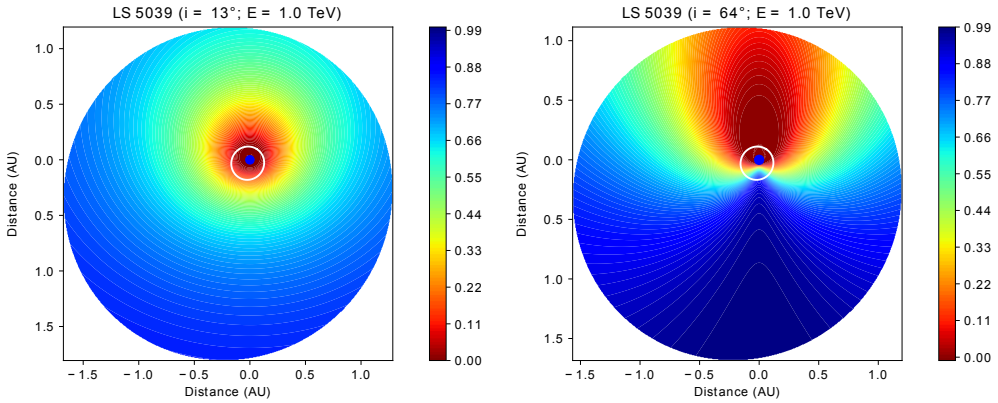

Figure 1: Absorption map for LS 5039, shown as $\exp(-\tau_{\gamma\gamma})$. The white line shows the orbit of the compact object, while the blue circle shows the O type companion star to scale ($R_\star = 9.3\,R_\odot$). The maps are calculated for an inclination of $i = 13°$ (left) and $i = 64°$ (right) which would correspond to a compact object in the mass range of a black hole or neutron star, respectively. The observer is at the bottom of the page.

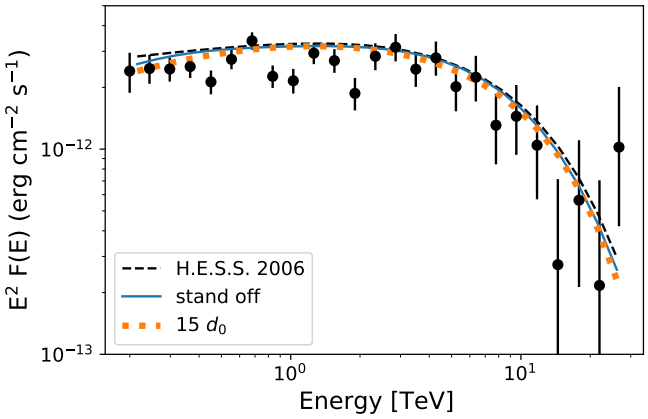

Figure 2: The modelled inverse Compton spectrum at inferior conjunction calculated at the stand-off shock (solid blue line) and at 15 times the binary separation (dotted orange line) compared to the observed very high energy spectrum between orbital phases $0.45 < \phi \leq 0.9$ (black points and dashed curve) [17].

figure 3. The gamma-gamma absorption at the shock should introduce a significant harder when fainter effect in the spectrum.

5. Discussion and Conclusions

The modelling of LS 5039 shows that if the emission is produced at the stand-off shock, there should be a significant absorption at ~ 1 TeV which should result in the hardening of the spectrum during the fainter states. These initial results do not take into account the full details of the particle acceleration and cooling, and the modelled flux, without absorption included, shows a slight harder when fainter trend, introduced by the change in the spectral shape due to the changing scattering angle. We have also not considered how systematic effects would influence the detection of the

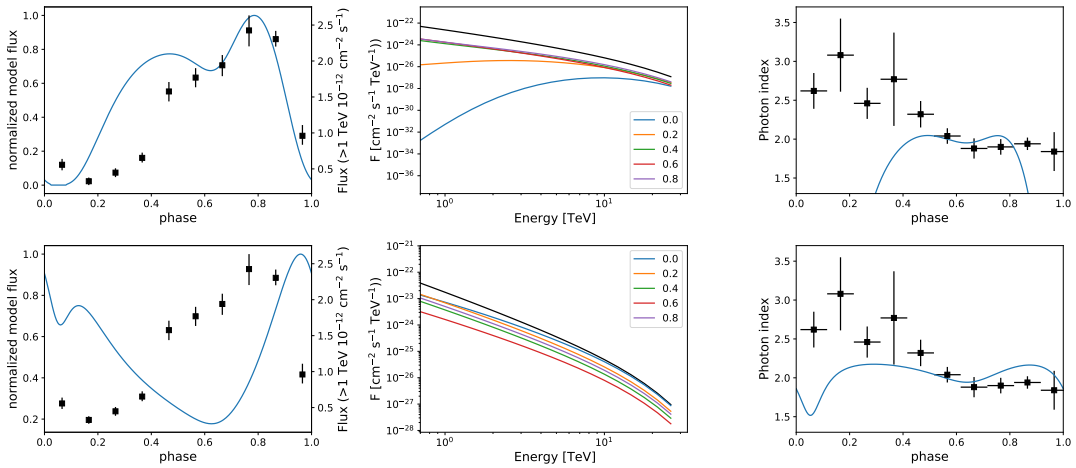

Figure 3: Modelled gamma-ray emission from LS 5039 at the stand-off shock (top row) and at 15 binary separations (bottom row). The modelled light curves curves are compared to the observed flux (left column); the change in the spectrum is shown for different phases, compared to the unabsorbed spectrum (black line; central column); while the modelled photon index (between 0.2 and 5 TeV) is compared to the observed photon index (right column). TeV observations from [17, 18], with phases adjusted to T_0 in [16].

photon spectrum. However, the results clearly show, that while the general shape of the modelled light curve is in approximate agreement with the observed light curves (however there is a poor fit around phase $\sim$ 0.4), there should be a significant hardening in the photon index that is not observed.

These initial results will be expanded to include other sources and investigated further. The change in the shape of the spectrum points to the possibility of using the future Cherenkov Telescope Array (CTA; [19]) to detect changes in the spectral energy distribution that may be able to constrain the location of the gamma-ray emission.

Acknowledgments

The numerical calculations were performed using the University of the Free State High Performance Computing Unit.

References

[1] G. Dubus, *Gamma-ray binaries and related systems*, A&A Rev. **21** (2013) 64 [1307.7083].

[2] M. Chernyakova, D. Malyshev, A. Paizis, N. La Palombara, M. Balbo, R. Walter et al., *Overview of non-transient γ-ray binaries and prospects for the Cherenkov Telescope Array*, A&A **631** (2019) A177 [1909.11018].

[3] S. Johnston, R.N. Manchester, A.G. Lyne, M. Bailes, V.M. Kaspi, G. Qiao et al., *PSR 1259-63 - A binary radio pulsar with a Be star companion*, ApJ **387** (1992) L37.

[4] F. Camilo, P.S. Ray, S.M. Ransom, M. Burgay, T.J. Johnson, M. Kerr et al., *Radio Detection of LAT PSRs J1741-2054 and J2032+4127: No Longer Just Gamma-ray Pulsars*, ApJ **705** (2009) 1 [0908.2626].

[5] G. Dubus, *Gamma-ray binaries: pulsars in disguise?*, A&A **456** (2006) 801 [astro-ph/0605287].

[6] M. Massi and F. Jaron, *Long-term periodicity in LS I +61°303 as beat frequency between orbital and precessional rate*, A&A **554** (2013) A105 [1303.2007].

[7] V. Bosch-Ramon, M.V. Barkov, D. Khangulyan and M. Perucho, *Simulations of stellar/pulsar-wind interaction along one full orbit*, A&A **544** (2012) A59 [1203.5528].

[8] G. Dubus, A. Lamberts and S. Fromang, *Modelling the high-energy emission from gamma-ray binaries using numerical relativistic hydrodynamics*, A&A **581** (2015) A27 [1505.01026].

[9] V. Zabalza, V. Bosch-Ramon, F. Aharonian and D. Khangulyan, *Unraveling the high-energy emission components of gamma-ray binaries*, A&A **551** (2013) A17 [1212.3222].

[10] M. Böttcher and C.D. Dermer, *Photon-Photon Absorption of Very High Energy Gamma Rays from Microquasars: Application to LS 5039*, ApJ **634** (2005) L81 [astro-ph/0508359].

[11] G. Dubus, *Gamma-ray absorption in massive X-ray binaries*, A&A **451** (2006) 9 [astro-ph/0509633].

[12] R.J. Gould and G.P. Schréder, *Pair Production in Photon-Photon Collisions*, *Physical Review* **155** (1967) 1404.

[13] D. Khangulyan, F.A. Aharonian and S.R. Kelner, *Simple Analytical Approximations for Treatment of Inverse Compton Scattering of Relativistic Electrons in the Blackbody Radiation Field*, ApJ **783** (2014) 100 [1310.7971].

[14] V. Zabalza, *Naima: a Python package for inference of particle distribution properties from nonthermal spectra*, in *34th International Cosmic Ray Conference (ICRC2015)*, vol. 34 of *International Cosmic Ray Conference*, p. 922, July, 2015 [1509.03319].

[15] J. Casares, M. Ribó, I. Ribas, J.M. Paredes, J. Martí and A. Herrero, *A possible black hole in the γ-ray microquasar LS 5039*, MNRAS **364** (2005) 899 [astro-ph/0507549].

[16] G.E. Sarty, T. Szalai, L.L. Kiss, J.M. Matthews, K. Wu, R. Kuschnig et al., *The γ-ray binary LS 5039: mass and orbit constraints from MOST observations*, MNRAS **411** (2011) 1293 [1009.5150].

[17] F. Aharonian, A.G. Akhperjanian, A.R. Bazer-Bachi, M. Beilicke, W. Benbow, D. Berge et al., *3.9 day orbital modulation in the TeV γ-ray flux and spectrum from the X-ray binary LS 5039*, A&A **460** (2006) 743 [astro-ph/0607192].

[18] C. Mariaud, P. Bordas, F. Aharonian, G. Dubus, M. Böttcher, M. de Naurois et al., *H.E.S.S. observations of LS 5039*, in *34th International Cosmic Ray Conference (ICRC2015)*, vol. 34 of *International Cosmic Ray Conference*, p. 885, July, 2015.

[19] M. Actis, G. Agnetta, F. Aharonian, A. Akhperjanian, J. Aleksić, E. Aliu et al., *Design concepts for the Cherenkov Telescope Array CTA: an advanced facility for ground-based high-energy gamma-ray astronomy*, *Experimental Astronomy* **32** (2011) 193 [1008.3703].